Iranian Journal of Catalysis 9(3), 2019, 259-268

IRANIAN JOURNAL OF CATALYSIS

Photocatalytic degradation of methyl orange using ZnO and Fe doped ZnO: A comparative study

Kalpesh Anil Isai[a,*], Vinod Shankar Shrivastava[b]

[a]*Department of Applied Sciences and Humanities, R.C. Patel Institute of Technology, Shirpur, (M.S.) India.*

[b]*Nano chemistry Research Laboratory, G. T. Patil College, Nandurbar, (M.S.) India.*

Received 16 February 2019; received in revised form 27 April 2019; accepted 5 May 2019

ABSTRACT

ZnO and 2% Fe doped ZnO photocatalytic nanomaterials were successfully synthesized by successive ionic layer adsorption and the reaction (SILAR) method. The characterizations of these nanomaterials were carried out using XRD, SEM and EDX techniques. XRD study shows that the samples have a hexagonal wurtzite crystal structure, size of which is in the range 21-23 nm. SEM shows nanoflakes or nano flower-like morphology, while EDX reveals the compositional analysis. In this paper, we investigated photocatalytic degradation of an aqueous suspension of methyl orange (MO) dye as a model pollutant. Degradation of dye was monitored by the spectrophotometric method. The effects of various parameters such as pH, contact time, initial dye concentration and catalyst dose were studied. in optimized process, the maximum degradation obtained using ZnO was 88 % and that using Fe doped ZnO was 94 % at a pH value of 8. We have concluded that, compared to ZnO, the 2% Fe doped ZnO is a promising photocatalyst for degradation of MO.

***Keywords**: Photocatalytic degradation, ZnO, Fe doped ZnO, Nanomaterial, MO.*

1. Introduction

Dyes are organic substances which can be absorbed by, made to react with, or deposited within a substrate and impart color to that substrate. Also, a dye is considered a colored and toxic substance [1]. The release of such hazardous dyes in the environment, due to rapid industrialization and population, is a major cause of water pollution. It is estimated that about 15% of the dye used cannot be recovered during dyeing processes and is released in wastewaters [2,3]. Wastewater having dyes is a dramatic source of pollution in the environment. In general, synthetic organic dyes are mostly used in the plastics, paper, textile, leather and cosmetic industries [4]. Strictly speaking, the dyes such as methyl orange (MO), methylene blue (MB), Congo red (CR), etc. used in textile industries for various processes contain azo compounds or groups [5]. Such azo groups are a serious threat to the environment due to their non-biodegradability [6]. Until now, various methods have been investigated to remove azo dyes [7-11].

*Corresponding author.
E-mail address: isai.kalpesh7@gmail.com (K.A. Isai)

But these methods cannot completely remove the contaminant dyes and the dyes are transformed into their toxic intermediates, which causes secondary pollution. So, to remove dyes or organic pollutants from industrial wastewater, a low cost and environment-friendly process for the complete conversion of pollutants needs to develop. Currently, photocatalysis can be used as the best technique for the degradation of dye pollutants. Photocatalysis is the process of speeding up of a photoreaction in the presence of a catalyst. In catalyzed photolysis, light is absorbed by an adsorbed substrate. In catalysis, the photocatalytic activity depends on the ability of the catalyst to create electron-hole pairs, which generate free radicals (e.g. hydroxyl radicals like $^{\bullet}OH$).

In the photocatalysis mechanism, the electron-hole pair was produced by the irradiation of a synthesized photocatalyst such as ZnO and 2% Fe doped ZnO with a photon of energy equal to or greater than its band gap width ($hv \geq Eg$). The electrons and holes may migrate to the catalyst surface where they participate in redox reactions with adsorbed species. Especially, hv^{+} may react with surface-bound H_2O or OH^{-} to produce the hydroxyl radical and e^{-}_{cb} is picked up by oxygen to

produce superoxide (O_2^-) radical anion. It has been suggested that these radicals are the primary oxidizing species in the photocatalytic oxidation processes as shown in the Eqs. (1-4) [12,13].

$$photocatalyst + hv \rightarrow e_{cb}^- + hv^+ \quad (1)$$

$$e_{cb}^- + O_{2(ads)} \rightarrow O_2{}^{-\cdot} \quad (2)$$

$$hv^+ + photocatalyst - OH \rightarrow HO_{ads}^* + H^+ \quad (3)$$

$$HO_{ads}^* + substrate \rightarrow photooxidized\ product \quad (4)$$

In general, the valence band contains a strongly oxidizing hole, while the conduction band contains strongly reducing electron. On the external surface of photocatalyst, the excited electrons and holes can take part in redox reactions with adsorbed species such as water, hydroxide (OH^-) ion, organics present in wastewater or oxygen. Generally, oxidation of water or OH^- by the hole produces the hydroxyl radical ($HO^{\bullet}$), these are extremely powerful and highly oxidant radicals (See supplementary data).

The positive-holes of metal oxide break apart water molecules to form hydrogen gas and hydroxyl radicals. The negative-electrons reacts with oxygen molecules to form superoxide anion and this cycle continues when light is available. In this way, it removes organics in the form of dyes in water [14,15]. The rapid recombination of photoinduced e^-/h^+ pairs has a major influence on the photocatalytic activity of the nanomaterials. Moreover, due to the wide band gap of ZnO, it does not have the ability to utilize the visible-light fraction of solar energy. Hence, different strategies have been used to overcome recombination of the photoinduced charge carriers and extend its optical response to the visible region. In recent years, it was found that doping is an effective modification [16]. So, in this work, we had made an effort to synthesize such a doped photocatalyst like Fe doped ZnO.

Photocatalysis can be used as the best method for the degradation of dye pollutants because it can mineralize organic dyes completely into H_2O, CO_2, and mineral acids without converting them into a secondary pollutant. A large number of cost-efficient, effective, and environment-friendly materials in the form of metal semiconductors are available and can overcome the environmental problems, such as TiO_2 [17], ZnO [18], Fe_2O_3 [19], CdS [20], and ZnS [21], etc. Among all such semiconductors, zinc oxide (ZnO) shows higher photocatalytic efficiency than others, it has been reported by various researchers [22,23].

ZnO is a typical n-type semiconductor, with a wide band gap of 3.37 eV and a high excitation binding energy of 60 meV [24]. Due to these important properties, it produces electron-hole pairs under UV or visible light irradiation. The interaction of these produced electrons and holes can reduce and oxidize the organic contaminants completely into their respective end products (CO_2 and H_2O, respectively) [25,26]. In recent years, research on ZnO and ZnO doped nanomaterials has paid more attention to the degradation of azo dye [27,28]. ZnO nanoparticles are synthesized by various techniques, such as hydrothermal synthesis [29], homogeneous precipitation [30], and SILAR method [31]. Except the SILAR method, these processes have many disadvantages, such as high expenses, costly equipment, large particle size, poor degradation capacity, etc. [32]. Among all these methods, the successive ionic layer adsorption and reaction (SILAR) method is relatively simple and offers a wide range of advantages over other expensive methods [33-35]; for example, this method produces uniform material, does not require any expensive and sophisticated instruments, and works at low operating temperature.

In this work, we have used a modified SILAR method to get ZnO and 2% Fe doped ZnO nanomaterial. It is a promising method because of its simplicity and low cost. The study aims to overcome the environmental challenge including industrial wastewater pollution; therefore, this work focuses on the synthesis of nanomaterials using SILAR and also their applications as a photocatalyst. Likewise, to promote interest in the SILAR method, it is applied for preparation of nanocrystalline metal oxide and doped metal oxide powders. For the photocatalytic degradation, we have used methyl orange (MO) dye as a model pollutant and examined its degradation using synthesized nanomaterials like ZnO and 2% Fe doped ZnO.

2. Experimental

2.1. Materials

All the chemicals used in the work were of analytical grade and all the solutions were prepared in distilled water. Chemicals used in this synthesis are zinc acetate dihydrate [$Zn(CH_3COO)_2{\cdot}2H_2O$], sodium hydroxide (NaOH), iron nitrate nonahydrate [$Fe(NO_3)_3{\cdot}9H_2O$], ethanol (C_2H_5OH) and distilled water. To study the photocatalytic activity, Methyl Orange dye was used as a model pollutant. The chemical structure and properties of MO are shown in supplementary data.

2.2. Method of Synthesis of Photocatalyst

2.2.1. Basic Mechanism of SILAR method

The basic mechanism of Successive Ionic Layer Adsorption and Reaction (SILAR) method has four

steps. These steps involve subsequent immersion of clean glass substrate in cationic and anionic solutions along with rinsing the substrate in double distilled water kept at room temperature. In general, this method was used for the synthesis of nano thin films, but here in this study, we make an attempt to prepare nanomaterial using this method.

The basic principle of SILAR method which was alternate dipping of the substrate in cationic and anionic precursors leads to the formation of a very weakly adherent film (powder precipitate) that could be easily scratched from the substrate and forms nanomaterial. SILAR method was followed by four different steps (See supplementary data) such as Adsorption, First rinsing (I), Reaction and Second rinsing (II) [36]. The first step was adsorption. The term 'adsorption' can be defined as a collection of substances on the surface of another substance. In this step, the cations present in the precursor solution are adsorbed on the surface of the substrate and form a double layer. This layer is composed of two layers, the inner (positively charged) and outer (negatively charged) layers. The positive layer consists of the cations and the negative form the counter ions of the cations. The second step was the first rinsing (I). In this step, loosely adsorbed ions are rinsed away from the diffusion layer. This results in a saturated double layer. The third step was the reaction, in which, the anions from the anionic precursor solution are introduced to the system. The fourth step was the second rinsing (II); in this step, the excess or unreacted species and the reaction byproduct from the diffusion layer are removed. By repeating these cycles, a thin layer of material can be grown.

By following the above-mentioned steps, the maximum increase in film thickness per one reaction cycle can theoretically create one monolayer then resulting in a solid layer of the compound. Thus, the process involves an alternate immersion of the substrate in a solution containing a soluble salt of the cation of the compound. The substrate supporting the growing film is rinsed in highly purified, deionized water after each immersion.

Compared to other nanomaterial synthesis processes, this simple process has low cost and temperature [37-41] so due to these advantages the SILAR process was used for the synthesis of ZnO and 2% Fe doped ZnO nanomaterials.

2.3. Synthesis and characterizations of nanoparticles

2.3.1. Substrate Cleaning

Initially, the glass substrate (6 cm × 1.25 cm × 1 mm) was washed with a detergent and then was kept in the chromic acid solution for 3 hours and was rinsed in distilled water and then for further cleaning, it was immersed in an equal volume of a mixture of acetone and alcohol in order to give a clean and rough surface for adsorption.

2.3.2. Synthesis of nanomaterials

Zinc acetate dehydrate [Zn $(CH_3COO)_2.2H_2O$] and sodium hydroxide (NaOH) were used as starting materials. In successive ionic layer adsorption and reaction (SILAR) method, cationic and anionic precursors were used for thin film deposition. For cationic precursor, the 0.1 M bath solution was prepared by slow addition of (0.2 M) 0.4 g sodium hydroxide (NaOH) into an aqueous solution of AR grade (0.1 M) 1.0975 g of zinc acetate dihydrate $[Zn(CH_3COO)_2.2H_2O]$. The pH of the cationic solution was adjusted to ~11 using NaOH or HCl while hot water (70 ℃) was used as an anionic precursor. Zinc oxide (ZnO) thin film was deposited on a well-cleaned glass substrate by using the SILAR process.

For the deposition of ZnO thin film, the substrate is initially immersed in a cationic precursor solution at about 20 seconds in which the zinc ions are absorbed by a substrate and then the substrate is rinsed in deionized water about 5 seconds. Thereafter, the substrate is immersed in the anionic precursor solution that is water for 20 seconds, which was kept at a constant temperature bath (about 70 ℃), the oxygen ions reacted with the adsorbed Zn^{2+} ions on the substrate. Finally, the glass substrate is immersed in deionized water for 5 seconds to remove the loosely bounded ions. One complete dipping cycle involves dipping the substrate in the cationic complex and then into the anionic complex. This completes one SILAR cycle for deposition of a ZnO thin film [42]. We prepared a thin film after 50 SILAR cycles manually and dried it at room temperature. This alternate dipping of the substrate in cationic and anionic precursors leads to a very weakly adherent ZnO film (powder precipitate) that could be easily scratched from the substrate (See supplementary data). Finally, by scraping off the powder from this prepared thin film, we got ZnO nanomaterial [43]. The powder was thoroughly washed 2-3 times with deionized water and dried at 50 ℃. Then, this dried powder was calcined at 100 ℃ to attain the suitable crystallinity or particle size.

The 2% Fe doped ZnO thin film was prepared by the cationic precursor; the cationic precursor was 0.1 M bath solution and it was prepared by the slow addition of (0.2 M) 0.4 g sodium hydroxide (NaOH) into an aqueous solution mixture (previously mixed solution) of AR grade (0.1 M) 1.0975 g of zinc acetate dihydrate $[Zn(CH_3COO)_2.2H_2O]$ and (0.1 M) 2.02 g of iron nitrate

nonahydrate [$Fe(NO_3)_3 \cdot 9H_2O$]. The pH of the cationic solution was obtained ~11 using NaOH or HCl, while hot water (70 ℃) was used as an anionic precursor. The similar procedure was carried out for the synthesis of 2% Fe doped ZnO nanomaterial.

2.3.3. Characterization of synthesized nanomaterials

XRD patterns of all nanomaterials were collected in the range of diffraction angle 2θ = 20°–80° using a Rigaku MiniFlex-600 diffractometer with Cu–Kα radiation at wavelength of 1.54056 Å. The surface morphology of the samples was studied using SEM Hitachi S-4800-Type-II (Hitachi High Technology Corporation) analysis at accelerating voltages of 20 kV. Elemental analysis and compositional analysis of the sample were carried out using Energy-dispersive X-ray Spectroscopy (EDXS), X-Flash detector 5030 and Bruker (Berlin, Germany).

2.4. Photocatalytic studies

2.4.1. Preparation of dye solution

The stock solution was prepared by dissolving MO dye in 100 mL of distilled water. To 10 mL of this stock solution, photocatalysts such as ZnO and 2% Fe doped ZnO were added. The aqueous solution was then magnetically stirred for half an hour and exposed to UV light. Similarly, the next desired concentration of dye solutions (20, 30, 40 and 50 mg/L) were prepared by diluting the stock solution with deionized water.

2.4.2. Photocatalytic degradation experiments

The photocatalytic degradation experiments were performed using the photocatalytic reactor (See supplementary data). The reactor contained a round and hollow Pyrex glass cell with 1.0 L limit, 10 cm breadth, and 15 cm height. For the light source, 150W mercury bulb was placed in a 5 cm width quartz tube with one end firmly fixed by a Teflon plug. The light and the tube were then submerged in the photoreactor cell with a light ray of 3.0 cm.

The photocatalytic activity of ZnO was evaluated with a photoreaction system using the degradation of MO under UV irradiation at room temperature. This UV irradiation was carried out using a 150W Hg bulb with the maximum emission wavelength at 464 nm. In a typical experiment, the photocatalyst was added to 50 mL of an aqueous solution containing a dye with the concentration of 10 mg/L (pH > 7, maintained by adding NaOH or HCl) placed in a beaker. Then, the solution was kept in the dark for 30 minutes at room temperature to reach the adsorption-desorption equilibrium of the dye on the ZnO surface before irradiation. The Hg bulb was turned on while the suspension of dye and photocatalyst was magnetically stirred, in order to degrade the dye. During this reaction, the distance between the solution surface and the light source was about 3.0 cm. At a fixed time interval, roughly 2-3 mL of sample was taken out for centrifugation at 10,000 rpm for 15 min, then the supernatant liquid was transferred into a spectrophotometer cell for measurement of the absorbance. An absorbance measurement was recorded using a UV-Vis spectrophotometer. Finally, the absorbance of the dye in the supernatant liquid was recorded by a UV spectrophotometer at the maximum absorption wavelength of the MO dye. a similar experiment for the next concentration solution was carried out and the absorptions were recorded. The % degradation of the dye can be calculated using Eq. 5.

$$\%\, Degradation = \frac{Co - Ct}{Co} \times 100 \qquad (5)$$

Where C_0 and C_t are the concentrations of the dye after self-photolysis and different irradiation times, respectively.

3. Results and Discussion

3.1. XRD analysis

XRD patterns as shown in Fig. 1 were used to characterize the crystal phases and crystallinity of the photocatalysts. It shows eleven different peaks at 2θ = 31.70º, 34.46º, 35.89º, 47.31º, 56.50º, 62.31º, 65.88º, 67.37º, 68.48º, 72.15º, 76.80º, match the planes [100], [002], [101], [102], [110], [103], [200], [112], [201], [004] and [202], which depict the hexagonal phase of ZnO [44]. Also 2% Fe doped ZnO shows eleven different peaks at 2θ = 31.48º, 34.05º, 35.80º, 47.49º, 56.54º, 62.40º, 65.83º, 67.42º, 68.60º, 72.10º, 76.55º, match the planes [100], [002], [101], [102], [110], [103], [200], [112], [201], [004] and [202], indicating the hexagonal phase of 2% Fe doped ZnO.

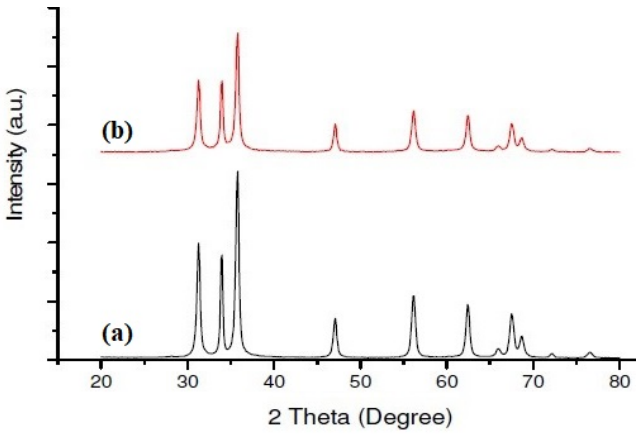

Fig. 1. XRD pattern of nanoparticles (a) ZnO (b) 2% Fe doped ZnO.

The data obtained showed a good agreement with the standard JCPDS card no. 36-1451 [45,46]. No any reflections of other phases were detected, this indicates that the prepared samples are of high purity. All XRD crystalline reflections of ZnO prepared also showed that the hexagonal wurtzite structure of ZnO. The average particle size of synthesized nanoparticles was calculated by using Scherer formula as shown in Eq. 6 and some changes in d values were observed from the data listed in supplementary data.

$$d = \frac{k\lambda}{\beta cos\theta} \qquad (6)$$

Where d, k, λ, β, and θ are the crystal size, Scherer constant (0.89), X-ray wavelength (0.154 nm), the peak full width at half maximum (FWHM), and the Bragg diffraction angle corresponding to ZnO [101] reflection.

The highest diffraction peaks were noted for three plane directions [100], [002], and [101]. The Fig. 1 (red-line XRD peaks) shows the progressive degradation of that peak and a slight increase in d-spacing with the increased Fe doping [47].

3.2. SEM and EDX analysis

The morphological and structural characterization of the prepared nanoparticles was investigated through SEM analysis. ZnO and 2% Fe doped ZnO show same the morphology as nanoflakes or nanoflowers shown in Fig. 2 (a and b) [48]. It also suggests that the synthesized nanoparticles have a crystalline structure with a large surface area. In photocatalytic reaction large surface is suitable for photocatalytic activity.

To confirm the purity of synthesized nanomaterial, EDX analysis was examined as demonstrated in Fig. 3 (a and b). Peaks assigned to Zn, Fe, and O were found, but no impurity peaks were detected; this further confirmed that the synthesized ZnO and 2% Fe doped ZnO were pure. The weight and atomic percentages of Zn and O are presented in Table 1.

3.3. Photocatalytic studies

The photocatalytic activity of the ZnO and 2% Fe doped ZnO was carried out under UV irradiation. UV-Vis absorption spectra showed a red shift in the doped sample compared to ZnO [49]. Doping of Fe shows high photocatalytic degradation compared to ZnO.

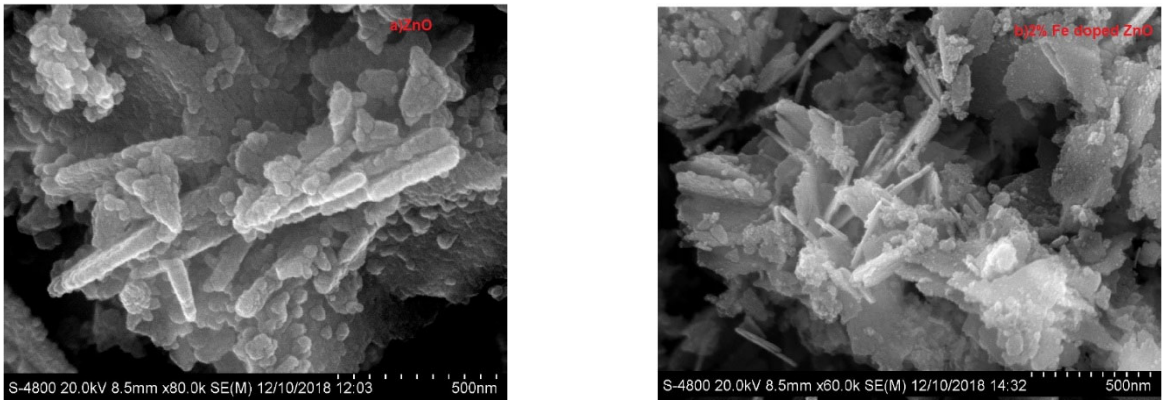

Fig. 2. SEM images of nanoparticles (a) ZnO (b) 2% Fe doped ZnO

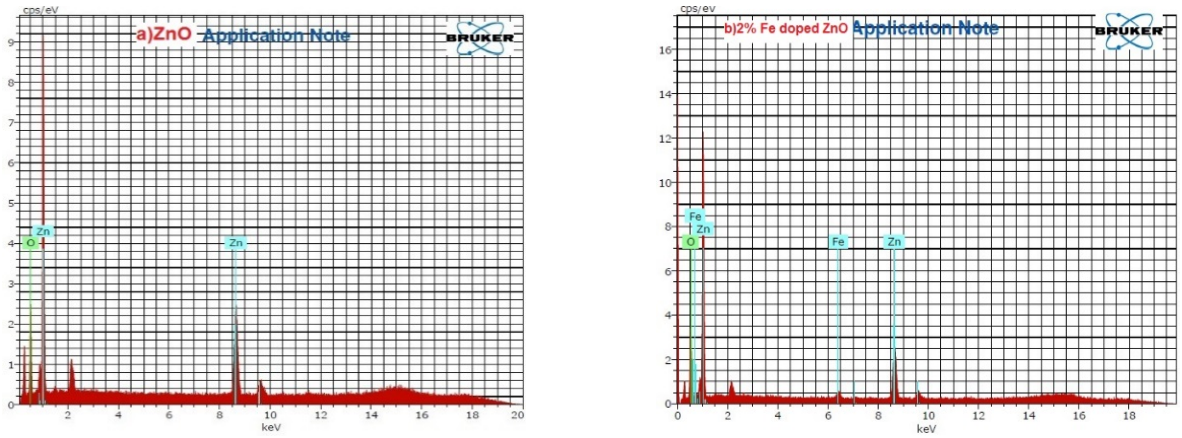

Fig. 3. EDX images of nanoparticles (a) ZnO (b) 2% Fe doped ZnO

Table 1. The atomic content of the nanoparticles obtained from the EDX analysis.

Type of nanoparticles	Elements	At %
ZnO	Zn K	54.92
	O K	45.08
2% Fe doped ZnO	Zn K	59.27
	O K	38.84
	Fe K	1.89

3.3.1. Effect of pH of the solution

pH plays an important role in the photocatalytic study. During the degradation of dye pH control reactions and also the generation of hydroxyl radicals depend on the pH of the solution [50]. Initially, the effect of pH was examined in the range of pH 2-10, it was adjusted using HCl and NaOH. As shown in Fig. 4, the conditions for optimizing pH were the catalyst dose of 1 g/L for the contact time of 180 minutes while the dye concentration was 20 mg/L. In general, the catalyst surface will be charged negatively when pH> pH_{zpc}, positively when pH< pH_{zpc} and neutrally when pH ≈ pH_{zpc}. The pH_{pzc} (point of zero charge) of the catalyst was estimated at about (ZnO=8.5 and 2% Fe doped ZnO = 8.1) using the reported method [51,52]. According to the pH_{pzc} values, the pH_{pzc} of ZnO was 8.5. It means at pH < 8.5, the ZnO surface has a net positive charge, while at pH > 8.5, the surface has a net negative charge, while the pH_{pzc} of 2% Fe doped ZnO was 8.1. It means at pH < 8.1, the surface has a net positive charge, while the pH > 8.1, the surface has a net negative charge [53].

As a result of pH_{pzc}, at alkaline pH, the catalyst surfaces were positively charged and so the negatively charged ions were attracted more towards the surface of the catalyst than the dye cation.

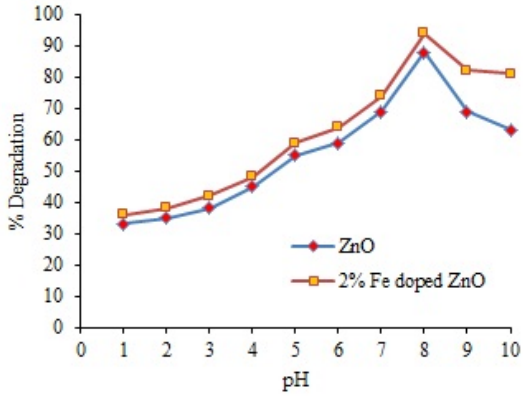

Fig. 4. Effect of pH on photocatalytic degradation of MO. Conditions: pH= 2-10, dye concentration 20 mg/L and (ZnO and 2% Fe doped ZnO) catalyst dose 1 g/L for the irradiation time 180 min.

Catalysts surfaces were negatively charged in an alkaline medium so that the dye cations were electrostatically attracted more towards the catalyst surface and thus, decoloration of MO dye was enhanced. The percentage of dye removal showed an increase when pH value increased and reached maximum value in the alkaline pH. Another reason for this observation was due to the increased generation of hydroxyl (•OH) radicals under alkaline conditions [54]. This study shows that by using ZnO and 2% Fe doped ZnO photocatalysts at pH 8 the maximum degradation of MO dye was found about 88 % and 94 %, respectively. So, pH 8 was chosen as the optimum pH and used for further experiments.

3.3.2. Effect of initial dye concentration

The effect of initial dye concentration at optimized pH 8 was examined by various initial dye concentrations. In this study, different initial concentrations of MO dye with a range of 10-50 mg/L were used to assess the photocatalytic activity. MO shows the maximum degradation at the 10 mg/L initial dye concentration, as shown in Fig. 5.

It is observed that the degradation efficiency of dye was decreased when the initial concentration of dye increased. Because as the initial dye concentration was increased indirectly, the excess of dye molecules will be adsorbed on the catalyst surface, so the active sites of the catalysts will be reduced. Also, the formation of hydroxyl (•OH) radicals on the catalyst surface remains constant for parameters such as the light intensity, catalyst dose and irradiation time. Indirectly, it lacks hydroxyl radicals for the degradation of MO dye at high concentrations [55]. From these results, 10 mg/L was chosen as the optimum initial dye concentration and used for further experiments.

3.3.3. Effect of contact time

During photocatalytic degradation of MO, the effect of contact time at optimum pH 8 and initial dye concentration of 10 mg/L were examined. The fixed amount of catalysts (ZnO and 2% Fe doped ZnO) used was 1 g/L. The relationships between the photocatalytic degradation of MO dye and the contact time of catalyst was investigated. The results are shown in Fig. 6. It was observed that when the irradiation time of catalyst increases, the degradation of MO improves [56]. Initially, due to the availability of a large number of active sites, the degradation rates till 100 min for ZnO and 140 min for 2% Fe doped ZnO, are faster, and after this time interval, it attains equilibrium. It means that at the time more than 100 min for ZnO and 140 min for 2% Fe doped ZnO, there will be repulsion between dye particles and catalyst surface, resulting in reduction of the degradation rate.

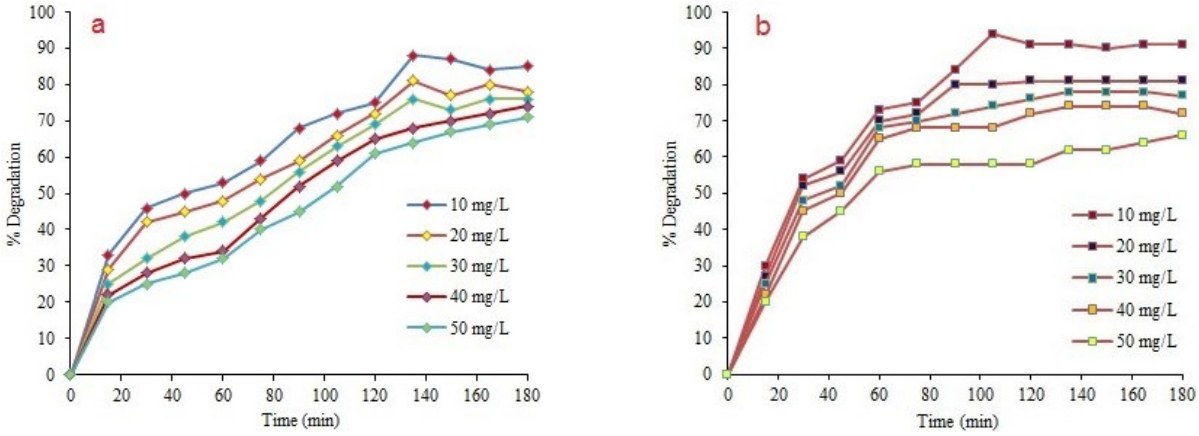

Fig. 5. Effect of initial dye concentration on the photocatalytic degradation of MO catalyzed by (a) ZnO and (b) 2% Fe doped ZnO. Conditions: pH=8, dye concentration 10, 20, 30, 40, 50 mg/L, (ZnO) and (2% Fe doped ZnO) catalyst dose 1 g/L for irradiation time 180 min.

3.3.4. Effect of catalyst dose

The effect of photocatalyst dose was studied at optimum conditions such as pH 8, initial dye concentration of 10 mg/L, contact time of 100 min for ZnO and 140 min for 2% Fe doped ZnO. Different catalyst doses of ZnO and 2% Fe doped ZnO were examined in the range 0.2–2 g/L. It is observed that the rate of degradation initially increases rapidly with the growth in catalyst concentration and thereafter decreases as shown in Fig. 7. Due to the catalyst concentration enhancement, the agglomeration (particle-particle interaction) also increases, and this is a major factor to reduce light absorption capacity of the photocatalyst. So, the degradation rate decreases as the catalyst dose increases. When the catalyst concentration is below this optimal value, it is assumed that the photocatalytic degradation is determined by the effective surface of the catalyst and the absorption of UV light. At lower catalyst loading, the absorption of light controls the photocatalytic process due to the limited catalyst surface. At higher catalyst loading, it can possibly have a negative effect by reducing the transitivity of light due to the formation of a milky solution, suggesting the need of an optimal amount of catalyst to balance the benefit of enhanced production of the active radicals and the light transitivity [57-60].

3.3.5. Kinetics study

The 2% Fe doped ZnO enhances the degradation efficiency as compared to ZnO. The photocatalytic degradation of MO dye using ZnO and 2% Fe doped ZnO follow the Pseudo-first order. At the low initial dye concentration, the rate expression is calculated by Eq. 7, [61].

$$\frac{d[C]}{dt} = k'C \qquad (7)$$

Where k' is the pseudo-first order rate constant. The dye was adsorbed on to the 2% Fe doped ZnO surface and the adsorption-desorption equilibrium reached.

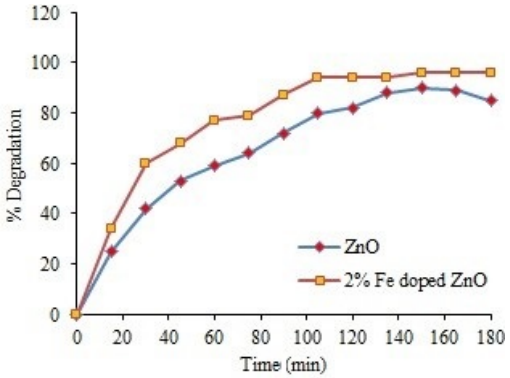

Fig. 6. Effect of contact time on photocatalytic degradation of MO. Conditions: pH=8, dye concentration 10 mg/L and catalyst dose 1 g/L, irradiation time 180 min.

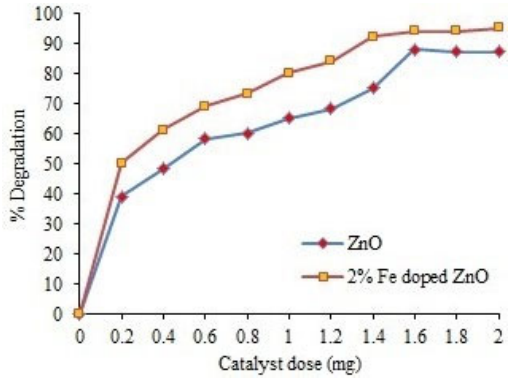

Fig. 7. Effect of catalyst dose on the photocatalytic degradation of MO. Conditions: pH=8, dye concentration 10 mg/L and catalyst dose 0.2-2 g/L, irradiation time 100 min for ZnO and 140 min for 2% Fe doped ZnO.

After adsorption, the equilibrium concentration of dye solution was determined and it is taken as the initial dye concentration for kinetic analysis. Integration of Eq. 7 (with the limit $C=C_0$ at $t=0$ with C_0 as the equilibrium concentration of the bulk solution) gives Eq. 8:

$$\ln(C_0/C) = k't \quad (8)$$

As can be seen, ln (C_0/C_t) is directly proportional to the contact time. The photocatalytic degradation of MO solution is directly proportional to the concentration. So, we can conclude that the photocatalytic degradation is the pseudo first order reaction. The apparent pseudo-first-order kinetic equation of ln (C_0/C_t) = k't [62] was used to fit experimental data. The linear transform in ln (C_0/C_t) as a function of contact time is given in Fig. 8 (a and b). This confirms that the kinetic curves were of apparent pseudo-first-order. The slope of the ln C_0/C_t vs the time plot gives the value of the rate constant k in min^{-1}. The rate constants obtained using ZnO nanomaterial are 0.01054, 0.00844, 0.00723 min^{-1} while using Fe doped ZnO are 0.01037, 0.00783, 0.00785 min^{-1}.

The photocatalytic activity can be compared to the k value and linear regression coefficient (R^2) for the MO solution with different initial concentrations, these data were summarized in Table 2. The k values are obtained by linear fitting from graph.

4. Conclusions

ZnO and 2% Fe doped ZnO photocatalysts were synthesized successfully by the SILAR method. The estimated particle size from XRD of the photocatalyst was to be about 21-23 nm. The 2% Fe doped ZnO photocatalyst shows high degradation efficiency at the low initial dye concentration and high catalyst dose as compared to ZnO. The process follows the pseudo-first-order kinetics with good correlation with the linear regression coefficient. This study shows that the degradation of MO was up to 88% using ZnO and was up to 94% using 2% Fe doped ZnO. It is concluded that, as compared to ZnO, the 2% Fe doped ZnO is a promising photocatalyst for degradation of MO.

Acknowledgments

Authors gratefully acknowledged the Principal, G.T.P. College, Nandurbar for providing necessary laboratory facilities. I am also thankful to the Department of Physics, Pratap College, Amalner for XRD facility and Central Instrumentation Laboratory, University Institute of Chemical Technology (UICT), N.M.U, Jalgaon, for providing FESEM and EDXS analysis facilities, the R.C. Patel Institute of Technology, Shirpur for promoting research work.

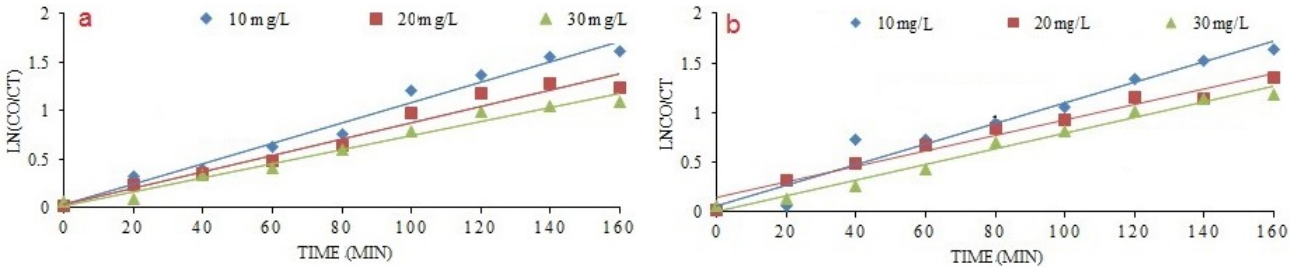

Fig. 8. Pseudo first order kinetics for photocatalytic degradation of MO, catalyzed by (a) ZnO and (b) 2% Fe doped ZnO. Conditions: pH=8, dye concentration 10, 20, 30 mg/L, (ZnO) catalyst dose 1 g/L for irradiation time 100 min and (2% Fe doped ZnO) catalyst dose 1 g/L for irradiation time 140 min.

Table 2. Pseudo first order rate constant of MO for photocatalytic degradation.

Catalyst	Amount of catalyst (g/L)	Conc. of dye (g/L)	Rate const., k, (min^{-1})	Linear regression coefficient (R^2)
ZnO	1 g/L	10	0.01054	0.9782
	1 g/L	20	0.00844	0.9663
	1 g/L	30	0.00723	0.9776
2% Fe doped ZnO	1 g/L	10	0.01037	0.9571
	1 g/L	20	0.00783	0.9727
	1 g/L	30	0.00785	0.9838

References

[1] D. Ayodhya, G. Veerabhadram, Mater. Today Energy 9 (2018) 83-113.
[2] L. Shabani, H. Aliyan, Iran. J. Catal. 6 (2016) 221-228.
[3] A. Buthiyappan, A. Raman Abdul Aziz, W. Mohd Ashri, W. Daud, Rev. Chem. Eng. 32 (2016) 1–47.
[4] M. Shahid, S. Islam, F. Mohammad, J. Clean. Prod. 53 (2013) 310-331.
[5] H.Y. Zhu, R. Jiang, Y.Q. Fu, Y.J. Guan, J. Yao, L. Xiao, Desalination 286 (2012) 41-48.
[6] N. Mathur, P. Bhatnagar, P. Sharma, Univers. J. Environ. Res. Technol. 2 (2012) 1-18.
[7] R. Kumar, G. Kumar, A. Umar, Mater. Lett. 97 (2013) 100-103.
[8] M. A. Chamjangali, G. Bagherian, B. Bahramian, B.F. Rad, Int. J. Environ. Sci. Technol. 12 (2015) 151–160.
[9] N.Z. Razali, A.H. Abdullah, M. Haron, Environ. Eng. Manag. J. 10 (2011) 1523-1528.
[10] N. Tripathy, R. Ahmad, J.E. Song, H.A. Ko, Y.B. Hahn, G. Khang, Mater. Lett. 136 (2014) 171-174.
[11] F. Tian, Z.S. Wu, Q.Y. Chen, Y.J. Yan, G. Cravotto, Z.L. Wu, Appl. Surf. Sci. 351 (2015) 104-112.
[12] A. Nezamzadeh-Ejhieh, H. Zabihi-Mobarakeh, J. Ind. Eng. Chem. 20 (2014) 1421–1431.
[13] H. Derikvandi, A. Nezamzadeh-Ejhieh, J. Colloid Interface Sci. 490 (2017) 314–327.
[14] K.M. Joshi, V.S. Shrivastava, Appl. Nanosci. 1 (2011) 147–155.
[15] M. Giahi, A. Hoseinpour Dargahi, Iran. J. Catal. 6 (2016) 381-387.
[16] M. Pirhashemi, A. Habibi-Yangjeh, Mater. Chem. Phys. 214 (2018) 107-119.
[17] D.D. Liu, Z.S. Wu, F. Tian, B.C. Ye, Y.B. Tong, J. Alloys Compd. 676 (2016) 489-498.
[18] S. Chidambaram, B. Pari, N. Kasi, S. Muthusamy, J. Alloys Compd. 665 (2016) 404-410.
[19] Y. Liu, L. Yu, Y. Hu, C.F. Guo, F.M. Zhang, X.W. Lou, Nanoscale 4 (2012) 183-187.
[20] A. Vázquez, D.B. Hernández-Uresti, S. Obregón, Appl. Surf. Sci. 386 (2016) 412-417.
[21] D. Pathania, D. Gupta, H. Ala, G. Sharma, A. Kumar, M. Naushad, J. Photochem. Photobiol. A 329 (2016) 61-68.
[22] H.J. Lee, J.H. Kim, S.S. Park, S.S. Hong, G.D. Lee, J. Ind. Eng. Chem. 25 (2015) 199–206.
[23] S.A. Ansari, M.M. Khan, M.O. Ansari, J. Lee, M.H. Cho, J. Phys. Chem. C 117 (2013) 27023-27030.
[24] N. Huang, J.X. Shu, Z.H. Wang, M. Chen, C.G. Ren, W. Zhang, J. Alloys Compd. 648 (2015) 919-929.
[25] M.M. Khan, J. Lee, M.H. Cho, J. Ind. Eng. Chem. 20 (2014) 1584-1590.
[26] S. Senapati, S.K. Srivastava, S.B. Singh, Nanoscale 4 (2012) 6604-6612.
[27] M. Thomas, G. Ahmad Naikoo, M. Ud Din Sheikh, M. Bano, F. Khan, J. Photochem. Photobiol. A 327 (2016) 33-43.
[28] S.P. Diego, L.D. Guilherme, A.M. Marcio, L.F. Edson, Global Nest J. 16 (2014) 690–698.
[29] K.D. Kim, D.N. Han, J.B. Lee, H.T. Kim, Scr. Mater. 54 (2006) 143-146.
[30] W.J. Li, E.W. Shi, Y.Q. Zheng, Z.W. Yin, J. Mater. Sci. Lett. 20 (2001) 1381-1383.
[31] M. Ristov, G. Sinadinovski, I. Grozdanov, M. Mitreski, Thin Solid Films 149 (1987) 65-71.
[32] A.A. Ismail, A. El-Midany, E.A. Abdel-Aal, H. El-Shall, Mater. Lett. 59 (2005) 1924-1928.
[33] R. Radha, A. Sakthivelu, D. Pradhabhan, C. Ravichandiran, S. Murugesan, E. Mohandas, P. Geethadhevi, Int. J. ChemTech Res. 6 (2014) 3374-3377.
[34] S. Lindroos, A. Arnold, M. Leskela, Appl. Surf. Sci. 158 (2000) 75-80.
[35] Y.F. Nicolau, M. Dupuy, M. Brunel, J. Electrochem. Soc. 137 (1990) 2915-2924.
[36] H.M. Pathan, C.D. Lokhande, Bull. Mater. Sci. 27 (2004) 85-111.
[37] T.A. Vijayan, R. Chandramohan, S. Valanarasu, J. Thirumalai, S. Venkateswaran, T. Mahalingam, S.R. Srikumar, Sci. Tech. Adv. Mater. 9 (2008) 1-5.
[38] K. Ramamoorthy, M. Arivanandhan, K. Sankaranarayanan, C. Sanjeeviraja, Mater. Chem. Phys. 85 (2004) 257-262.
[39] P. Mitra, A.P. Chatterjee, H.S. Maiti, J. Mater. Sci. 9 (1998) 441-445.
[40] A. Sakthivelu, S. Valanarasu, J. Joseph Prince, Int. J. Chem. Sci. 7 (2009) 2463-2469.
[41] P. Mitra, S. Mondal, Prog. Theor. Appl. Phys. 1 (2013) 17-31.
[42] A.P. Chatterjee, P. Mitra, A.K. Mukhopadhyay, J. Mater. Sci. 34 (1999) 4225-4231.
[43] S. Patra, S. Mondal, P. Mitra, J. Phys. Sci. 13 (2009) 229-234.
[44] S. Aghdasi, M. Shokri, Iran. J. Catal. 6 (2016) 481-487.
[45] R. Kumar, G. Kumar, A. Umar, Mater. Lett. 97 (2013) 100-103.
[46] S. Aiswarya Devi, M. Harshiny, S. Udaykumar, P. Gopinath, M. Matheswaran, Toxicol. Res. 6 (2017) 854-865.
[47] M. Salem, S. Akir, T. Ghrib, K. Daoudi, M. Gaidi, J. Alloys Compd. 685 (2016) 107-113.
[48] J. Xie, P. Li, Y. Wang, Y. Wei, J. Phys. Chem. Solids 70 (2009) 112-116.
[49] M. Bordbara, Z. Sayban, A. Yeganeh-Faal, B. Khodadadi, Iran. J. Catal. 8 (2018) 113-120.
[50] S. Sakthivel, B. Neppolian, M.V. Shankar, B. Arabindoo, M. Palanichamy, V. Murugesan, Sol. Energy Mater. Sol. Cells 77 (2003) 65-82.
[51] M. Omar Fatehah, H. Abdul Aziz, S. Stoll, J. Colloid Sci. Biotechnol. 3 (2014) 75-84.
[52] A. Eslami, A. Oghazyan, M. Sarafraz, Iran. J. Catal. 8 (2018) 95-102.
[53] M. Farrokhi, S. Hosseini, J. Yang, M. Shirzad-Siboni, Water Air Soil Pollut. 225 (2014) 1-12.

[54] A.H. Mahvi, M. Ghanbarian, S. Nasseri, A. Khairi, Desalination 239 (2009) 309-316.
[55] S.D. Khairnar, M.R. Patil, V.S. Shrivastava, Iran. J. Catal. 8 (2018) 143-150.
[56] L.A. Ghule, A.A. Patil, K.B. Sapnar, S.D. Dhole, K.M. Garadkar, Toxicol. Environ. Chem. 93 (2011) 623–634.
[57] T.E. Agustina, H.M. Ang, V.K. Pareek, J. Photochem. Photobiol. C 6 (2005) 264–273.
[58] H. Wang, C. Xie, W. Zhang, S. Cai, Z. Yang, Y. Gui, J. Hazard. Mater. 141 (2007) 645-652.
[59] S. Vadaei, H. Faghihian, Environ. Toxicol. Pharmacol. 58 (2018) 45-53.
[60] A. Nezamzadeh-Ejhieh, M. Karimi-Shamsabadi, Appl. Catal. A 477 (2014) 83–92.
[61] N. Sobana, B. Krishnakumar, M. Swaminathan, Mater. Sci. Semicond. Process. 16 (2013) 1046-1051.
[62] V. Djokić, J. Vujović, A. Marinković, R. Petrović, D. Janaćković, A. Onjia, D. Mijin, J. Serbian Chem. Soc. 77 (2012) 1747-1757.